



1 Atmospheric Oxidation Mechanism and Kinetics of Indole Initiated 2 by $\cdot\text{OH}$ and $\cdot\text{Cl}$: A Computational Study

3 Jingwen Xue^{1#}, Fangfang Ma^{1*}, Jonas Elm², Jingwen Chen¹, Hong-Bin Xie^{1*}

4 ¹Key Laboratory of Industrial Ecology and Environmental Engineering (Ministry of Education), School of Environmental
5 Science and Technology, Dalian University of Technology, Dalian 116024, China

6 ²Department of Chemistry and iClimate, Aarhus University, Langelandsgade 140, DK-8000 Aarhus C, Denmark

7 *Correspondence to:* Fang-Fang Ma (maff@dlut.edu.cn); Hong-Bin Xie (hbxie@dlut.edu.cn)

8 **Abstract.** The atmospheric chemistry of organic nitrogen compounds (ONCs) is of great importance for understanding the
9 formation of carcinogenic nitrosamines and ONC oxidation products might influence atmospheric aerosol particle formation
10 and growth. Indole is a polyfunctional heterocyclic secondary amine with global emission quantity almost equivalent to that
11 of trimethylamine, the amine with the highest atmospheric emission. However, the atmospheric chemistry of indole remains
12 unclear. Herein, the reactions of indole with $\cdot\text{OH}/\cdot\text{Cl}$, and subsequent reactions of resulting indole-radicals with O_2 under 200
13 ppt NO and 50 ppt $\text{HO}_2\cdot$ conditions, were investigated by a combination of quantum chemical calculations and kinetics
14 modeling. The results indicate that $\cdot\text{OH}$ addition is dominant pathway for the reaction of $\cdot\text{OH}$ with indole. However, both $\cdot\text{Cl}$
15 addition and H-abstraction are feasible for the corresponding reaction with $\cdot\text{Cl}$. All favorably formed indole-radicals further
16 react with O_2 to produce peroxy radicals, which mainly react with NO and $\text{HO}_2\cdot$ to form organonitrates, alkoxy radicals and
17 hydroperoxide products. Therefore, the oxidation mechanism of indole is distinct from that of previously reported amines,
18 which primarily form highly oxidized multifunctional compounds, imines or carcinogenic nitrosamines. In addition, the peroxy
19 radicals from the $\cdot\text{OH}$ reaction can form N-(2-formylphenyl)formamide ($\text{C}_8\text{H}_7\text{NO}_2$), for the first time providing evidence for
20 the chemical identity of the $\text{C}_8\text{H}_7\text{NO}_2$ mass peak observed in the $\cdot\text{OH}$ + indole experiments. More importantly, this study is
21 the first to demonstrate despite forming radicals by abstracting an H-atom at the N-site, carcinogenic nitrosamines were not
22 produced in the indole oxidation reaction.

23 1 Introduction

24 Volatile organic compounds (VOCs) play a central role in air quality and climate change as their transformations are
25 highly relevant for the formation of secondary organic aerosols (SOA), toxic air pollutants and ozone (O_3) (Ehn et al., 2014;
26 Karl et al., 2018; Lewis Alastair, 2018; Li et al., 2019; Khare and Gentner, 2018; Ji et al., 2018). Therefore, an accurate
27 description of the atmospheric transformation mechanism and kinetics of VOCs is essential to fully explore the global impacts
28 of VOCs. Despite massive effort to understand the atmospheric fate of VOCs, current mechanism-based atmospheric models
29 often underestimate SOA and O_3 formation quantity. Therefore, the emission inventories or reaction mechanism employed in



30 the models are either missing some vital primary VOCs or there remain unrevealed reaction mechanism of currently known
31 VOCs. Hence, it is crucial to identify unaccounted reaction pathways of known VOCs or transformation mechanism of
32 unconsidered VOCs with high concentrations.

33 Organic nitrogen compounds (ONCs) are a subgroup of VOCs that are widely observed in the atmosphere (Silva et al.,
34 2008). Until now, about 160 ONCs have been detected in the atmosphere, accounting for 10% of total gas phase nitrogen (Ge
35 et al., 2011; Silva et al., 2008). Due to the adverse effects of ONCs on air quality (formation of particles via acid-base reactions
36 or generation of toxic nitrosamines, nitramines, isocyanic acid and low volatile products via gas phase oxidation), the chemistry
37 of ONCs has gained significant attention in the recent years (Almeida et al., 2013; Chen et al., 2017; Lin et al., 2019; Nielsen
38 et al., 2012; Zhang et al., 2015; Xie et al., 2014; Xie et al., 2015; Xie et al., 2017; Ma et al., 2018a; Ma et al., 2021a; Ma et al.,
39 2019; Shen et al., 2019; Shen et al., 2020). Detailed transformation pathways of a series of ONCs including low-molecular-
40 weight alkyl amines (Nicovich et al., 2015; Xie et al., 2014; Xie et al., 2015; Ma et al., 2021a), aromatic aniline (Xie et al.,
41 2017; Shiels et al., 2021), heterocyclic amines (Sengupta et al., 2010; Ma et al., 2018a; Borduas et al., 2016; Ren and Da Silva,
42 2019) and amides (Xie et al., 2017; Borduas et al., 2016; Borduas et al., 2015; Bunkan et al., 2016; Bunkan et al., 2015) have
43 been investigated. These studies have shown that the functional groups connected to the NH_x ($x = 0, 1, 2$) group highly affect
44 the reactivity of ONCs and eventually lead to their different atmospheric impacts. Therefore, the comprehensive understanding
45 the reaction mechanism of ONCs with various functional groups linked to the NH_x group is of great significance to assess the
46 atmospheric impact of ONCs.

47 Indole is a polyfunctional heterocyclic secondary amine (Laskin et al., 2009). Atmospheric indole has various natural and
48 anthropogenic sources including vegetation, biomass burning, animal husbandry, coal mining, petroleum processing and
49 tobacco industry (Ma et al., 2021b; Cardoza et al., 2003; Yuan et al., 2017; Zito et al., 2015). The global emission of indole is
50 around 0.1 Tg yr^{-1} (Misztal et al., 2015), which is almost equivalent to that of trimethylamine ($\sim 0.17 \text{ Tg yr}^{-1}$) (Schade and
51 Crutzen, 1995; Yu and Luo, 2014) which has the highest emission among the identified atmospheric amines. A field
52 measurement study found that the concentration of indole can reach 1-3 ppb in ambient air during a springtime flowering event
53 (Gentner et al., 2014). From a structural point of view, the -NH- group of indole is located at 9-center-10-electron delocalized
54 π bonds, possibly altering its reactivity compared to that of previously well-studied aliphatic amines and aniline. Therefore,
55 considering the large atmospheric emission of indole and its unique structure compared to previously studied amines, the
56 reaction mechanism of indole needs to be further evaluated to assess its atmospheric impacts. Furthermore, elucidating the
57 reaction mechanism of indole will add to the fundamental understanding of the transformation mechanism of ONCs.

58 Hydroxyl radicals ($\cdot\text{OH}$) are considered to be the most important atmospheric oxidants governing the fate of most organic
59 compounds (Macleod et al., 2007). Previous experimental studies have investigated the reaction kinetics (k_{OH}) and identified
60 the products of the $\cdot\text{OH} + \text{indole}$ reaction. Atkinson et al. found that the k_{OH} value of the $\cdot\text{OH} + \text{indole}$ reaction is 1.54×10^{-10}
61 $\text{cm}^3 \text{ molecule}^{-1} \text{ s}^{-1}$ at 298 K, translating to a 20 min lifetime of indole (Atkinson et al., 1995). Montoya-Aguilera et al. found
62 that isatin and isatoic anhydride are the two dominate monomeric products for $\cdot\text{OH}$ initiated reaction of indole. More
63 importantly, they found that the majority of indole oxidation products can contribute to SOA formation with an effective SOA



64 yield of 1.3 ± 0.3 under the indole concentration (200 ppb) employed in their chamber study (Montoya-Aguilera et al., 2017).
65 Although the chemical formulas of some of the indole oxidation products have been detected, detailed mechanistic information
66 such as the products branching ratio of the $\cdot\text{OH}$ initiated reaction of indole remains unknown. Additionally, the lack of
67 commercially available standards of some products presents a significant obstacle to identify the exact chemical identity of the
68 products. Therefore, to fully understand the role of indole in SOA formation, it is essential to investigate the detailed
69 atmospheric transformation of indole initiated by $\cdot\text{OH}$.

70 Besides reactions with $\cdot\text{OH}$, reactions with chlorine radicals ($\cdot\text{Cl}$) have been proposed to be an important removal pathway
71 for ONCs due to the identification of new $\cdot\text{Cl}$ continental sources and the high reactivity of $\cdot\text{Cl}$ (Wang et al., 2022; Li et al.,
72 2021; Jahn et al., 2021; Xia et al., 2020; Young et al., 2014; Faxon and Allen, 2013; Riedel et al., 2012; Atkinson et al., 1989;
73 Ji et al., 2013; Thornton et al., 2010; Le Breton et al., 2018). $\cdot\text{Cl}$ initiated atmospheric oxidation of ONCs can lead to the
74 formation of N-centered radicals, once a strong 2-center-3-electron (2c-3e) bond complex has been formed between $\cdot\text{Cl}$ and
75 NH_x ($x = 1, 2$). (Mckee et al., 1996; Xie et al., 2015; Xie et al., 2017; Ma et al., 2018a). The formed N-centered radicals can
76 further react with NO to form carcinogenic nitrosamines, increasing the atmospheric impact of ONC emissions (Xie et al.,
77 2014; Xie et al., 2015; Xie et al., 2017; Ma et al., 2018a; Ma et al., 2021a; Onel et al., 2014a; Onel et al., 2014b; Nielsen et al.,
78 2012; Da Silva, 2013). As a secondary amine, indole reactions with $\cdot\text{Cl}$ has the possibility of forming N-centered radicals and
79 subsequently forming nitrosamines via the reaction with NO. Since the $-\text{NH}-$ group of indole is embedded in a unique chemical
80 environment compared to previously well-studied ONCs, the reaction mechanism of $\cdot\text{Cl}$ with indole remain elusive. In addition,
81 there are only a few studies concerning the reactions of polyfunctional heterocyclic ONCs with $\cdot\text{Cl}$.

82 In this work, we investigated the reaction mechanism and kinetics of indole initiated by $\cdot\text{OH}$ and $\cdot\text{Cl}$ by employing a
83 combination of quantum chemical calculations and kinetic modeling. The initial reactions of $\cdot\text{OH}/\cdot\text{Cl} + \text{indole}$ and the
84 subsequent reactions with O_2 of resulting intermediates were further investigated.

85 **2 Computational Details**

86 **2.1 Ab Initio Electronic Structure Calculations**

87 All the geometry optimizations and harmonic vibrational frequency calculations were performed at the M06-2X/6-
88 31+G(d,p) level of theory (Zhao and Truhlar, 2008). Intrinsic reaction coordinate calculations were performed to confirm the
89 connections of each transition state between the corresponding reactants and products. Single point energy calculations were
90 performed at the CBS-QB3 method based on the geometries at the M06-2X/6-31+G(d,p) level of theory (Montgomery et al.,
91 1999). The combination of the M06-2X functional and CBS-QB3 method has successfully been applied to predict radical-
92 molecule reactions (Guo et al., 2020; Ma et al., 2021b; Wang et al., 2018; Wang and Wang, 2016; Wu et al., 2015; Wang et al.,
93 2017; Fu et al., 2020). T_1 diagnostic (Table S2) values in the CCSD(T) calculations within the CBS-QB3 scheme for the
94 intermediates and transition states involved in the key reaction pathways were checked for multireference character. The T_1
95 diagnostic values for all checked important species in this work are lower than the threshold value of 0.045, indicating the



96 reliability of applied single reference methods (Rienstra-Kiracofe et al., 2000). In addition, similar to our previous studies, a
97 literature value of $0.8 \text{ kcal mol}^{-1}$ for the isolated $\cdot\text{Cl}$ was used to account for the effect of spin-orbit coupling in the $\cdot\text{Cl} + \text{indole}$
98 reaction (Nicovich et al., 2015; Xie et al., 2017; Ma et al., 2018a). Atomic charges of indole and pre-reactive complexes in
99 the $\cdot\text{Cl} + \text{indole}$ reaction are obtained by natural bond orbital (NBO) calculations (Reed et al., 1985). All calculations were
100 performed within the Gaussian 09 package (Frisch et al., 2009). Throughout the paper, the symbols “R, RC, PC, TS, IM and
101 P” stand for reactants, pre-reactive complexes, post-reactive complexes, transition states, intermediates and products involved
102 in the reactions, respectively, and their subscripts denote different species. In addition, “A/B” was used to present the
103 computational method, where “A” is the theoretical level for single point energy calculations and “B” is that for geometry
104 optimizations and harmonic frequency calculations.

105 2.2 Kinetics Calculations

106 The reaction rate constants for the reactions of $\cdot\text{OH}/\cdot\text{Cl} + \text{indole}$ and the subsequent reactions of resulting primary
107 intermediates were performed with the MultiWell-2014.1 and MESMER 5.0 program (Barker and Ortiz, 2001; Barker, 2001;
108 Glowacki et al., 2012), respectively. For the reactions with tight transition states, the Rice-Ramsperger-Kassel-Marcus (RRKM)
109 theory within the MultiWell-2014.1 or MESMER 5.0 program was used to calculate the reaction rate constants based on
110 energies and structures at the CBS-QB3//M06-2X/6-31+G(d,p) level of theory (Holbrook, 1996; Robinson, 1972). For
111 barrierless entrance pathways (from R to RC), the long-range transition-state theory (LRTST) with a dispersion force potential
112 within the MultiWell-2014.1 program (Barker and Ortiz, 2001) or Inverse Laplace Transformation (ILT) method within the
113 MESMER 5.0 program was employed to calculate the reaction rate constants (Rienstra-Kiracofe et al., 2000). Computational
114 details for performing LRTST and ILT calculation were described in our previous studies (Ma et al., 2021a; Ma et al., 2021b;
115 Guo et al., 2020; Ding et al., 2020b). The parameters used in the LRTST calculations and Lennard-Jones parameters of
116 intermediates estimated by the empirical method proposed by Gilbert and Smith (Gilbert, 1990) are listed in Table S3 and
117 Table S4, respectively. N_2 was selected as the buffer gas, and an average transfer energy of $\Delta E_d = 200 \text{ cm}^{-1}$ was used to
118 simulate the collision energy transfer between active intermediates and N_2 . For the reactions involving H-abstraction or H-
119 shift, tunneling effects were taken into account in all of the reaction rate constants calculations by using a one-dimensional
120 unsymmetrical Eckart barrier (Eckart, 1930), and were discussed in Supporting Information (SI).

121 3 Results and Discussion

122 3.1 Initial Reactions of Indole

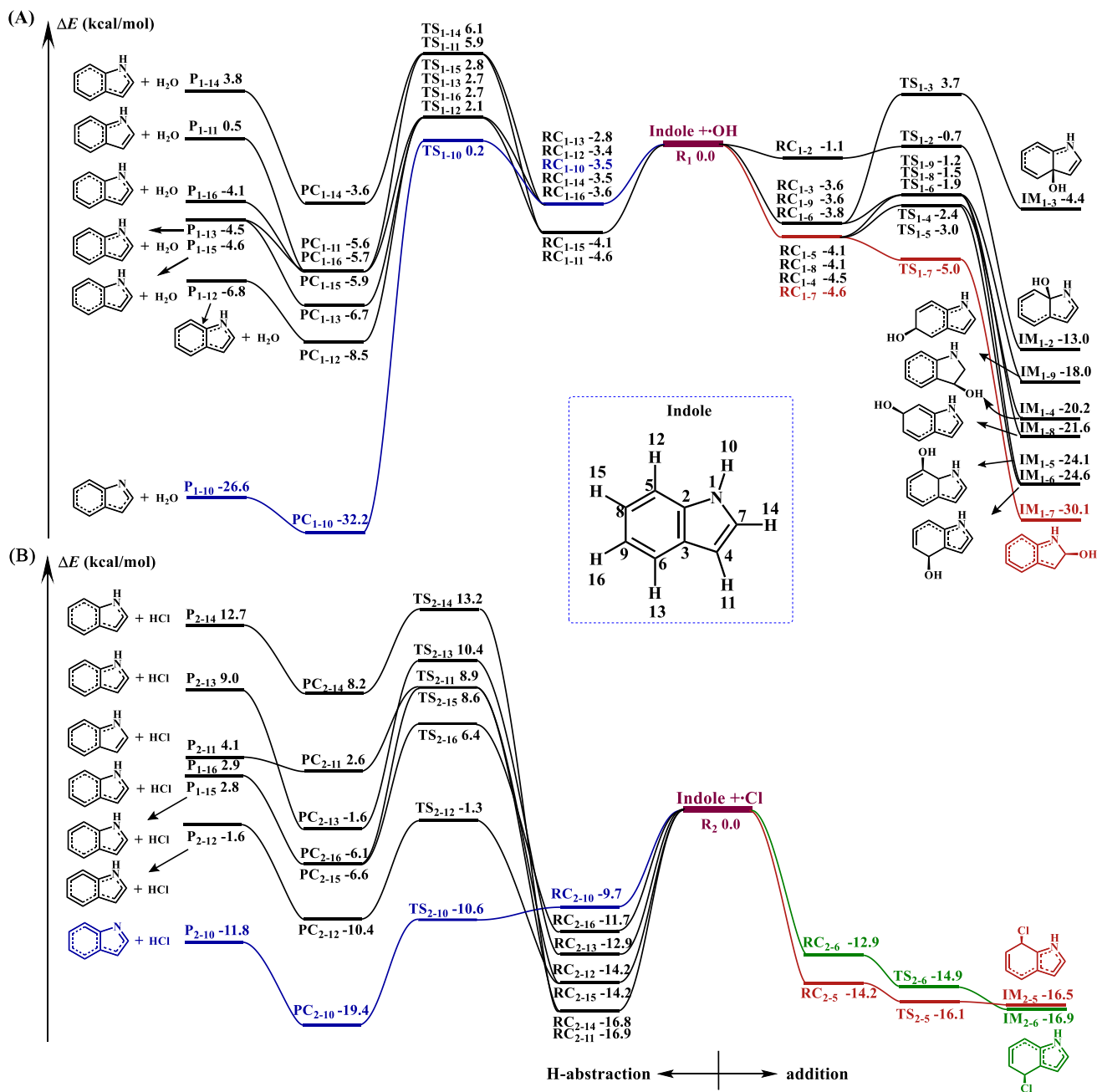
123 In principle, $\cdot\text{OH}$ and $\cdot\text{Cl}$ could add to the unsaturated $\text{C}=\text{C}$ bonds and phenyl group or directly abstract H-atoms
124 connected to either to a C-atom or the N-atom of indole. Considering the planar C_s structure of indole, $\cdot\text{OH}$ and $\cdot\text{Cl}$ addition
125 to one side of indole was only considered here. However, although numerous attempts have been made, we failed to locate the
126 TSs and addition IMs of $\cdot\text{Cl}$ addition to the C2, C3, C4, C7, C8 and C9 sites of indole, suggesting that such additions are in



127 fact unfeasible. Therefore, 7 H-abstraction pathways of $\cdot\text{OH}$ and $\cdot\text{Cl}$, respectively, 8 $\cdot\text{OH}$ -addition pathways and 2 $\cdot\text{Cl}$ -addition
128 pathways were considered for the $\cdot\text{OH}/\cdot\text{Cl} + \text{indole}$ reactions. The schematic zero-point energy (ZPE) corrected potential
129 energy surfaces of $\cdot\text{OH}/\cdot\text{Cl} + \text{indole}$ reactions are presented in Figure 1.

130 As can be seen from Figure 1, each H-abstraction reaction pathway proceeds through a RC and PC, and the addition
131 pathways through a RC for the $\cdot\text{OH}/\cdot\text{Cl} + \text{indole}$ reactions. For the H-abstraction pathways, the activation energy (E_a) for the
132 $-\text{NH}-$ group for both reactions are at least $2.0 \text{ kcal mol}^{-1}$ lower than the corresponding E_a values for the $-\text{CH}-$ groups. This
133 indicates that H-abstraction from the $-\text{NH}-$ group forming $\text{C}_8\text{H}_6\text{N}$ radicals and $\text{H}_2\text{O}/\text{HCl}$ is the most favorable among all the
134 H-abstraction pathways. In addition, the activation energy for the H-abstraction from the $-\text{NH}-$ group in the $\cdot\text{Cl} + \text{indole}$
135 reaction is much lower than the corresponding $\cdot\text{OH} + \text{indole}$ reaction. This is consistent with previously reported reactions of
136 other amines with $\cdot\text{OH}$ and $\cdot\text{Cl}$ (Ma et al., 2018a; Ma et al., 2021a; Xie et al., 2014; Xie et al., 2015; Xie et al., 2017; Tan et
137 al., 2021; Ren and Da Silva, 2019; Borduas et al., 2015).

138 For the addition reactions, the most favorable reaction site differs for the indole + $\cdot\text{OH}$ and indole + $\cdot\text{Cl}$ reactions. Among
139 all 8 $\cdot\text{OH}$ addition pathways, $\cdot\text{OH}$ addition to the C7 site of the $\text{C}=\text{C}$ bond via $\text{TS}_{1.7}$ forming $\text{IM}_{1.7}$ is the most favorable
140 pathway. Different from the reaction with $\cdot\text{OH}$, the additions of $\cdot\text{Cl}$ to the C5 and C6 sites to form $\text{IM}_{2.5}$ and $\text{IM}_{2.6}$, respectively,
141 are significantly more favorable. By comparing the E_a values of the addition and H-abstraction pathways for both $\cdot\text{OH}/\cdot\text{Cl} +$
142 indole reactions, it can be concluded that $\cdot\text{OH}$ addition to the C7 site is the most favorable for the $\cdot\text{OH} + \text{indole}$ reaction. All
143 the $\cdot\text{OH} + \text{indole}$ hydrogen abstraction reactions have high energy barriers. However, the additions of $\cdot\text{Cl}$ to the C5 and C6
144 sites as well as the $-\text{NH}-$ H-abstraction are all favorable due to their very lower E_a values for the $\cdot\text{Cl} + \text{indole}$ reaction.



145

146 **Figure 1: Schematic ZPE-corrected potential energy surface for the reactions of indole + $\cdot\text{OH}$ (A) and indole + $\cdot\text{Cl}$ (B)**
 147 **at the CBS-QB3//M062X/6-31+g(d,p) level of theory. The total energy of the reactants indole + $\cdot\text{OH}/\cdot\text{Cl}$ are set to zero,**
 148 **respectively (reference state).**

149 Interestingly, we found that all the pathways for the indole + $\cdot\text{Cl}$ reaction can proceed via a stable 2c-3e bonded RC,
 150 which is different from that of the $\cdot\text{OH}$ + indole reaction. Among all 2c-3e bonded RCs, only RC_{2-10} from the -NH- abstraction
 151 pathway is formed between the N-atom and $\cdot\text{Cl}$, while the others are formed between the C-atom and $\cdot\text{Cl}$. Note that RC_{2-11} ,



152 which forms from C-atom and $\cdot\text{Cl}$, is the most stable among all the formed RCs in the $\cdot\text{Cl}$ + indole reaction. To the best of our
153 knowledge, this is the first time that such a stable 2c-3e bonded RC has been identified between the C-atom and $\cdot\text{Cl}$. In addition,
154 the energy of RC₂₋₁₀ is higher than that of the traditional 2c-3e bonded RCs formed from alkylamine and $\cdot\text{Cl}$, which would
155 result from the delocalization of lone pair electrons of the N-atom. By analyzing the NBO charges of these nine RCs (Table
156 S3), we found that significant charge transfer occurs between $\cdot\text{Cl}$ and indole. The charge at Cl atom for RC₂₋₅, RC₂₋₆, RC₂₋₁₀,
157 RC₂₋₁₁, RC₂₋₁₂, RC₂₋₁₃, RC₂₋₁₄, RC₂₋₁₅ and RC₂₋₁₆ are $-0.35 e$, $-0.33 e$, $-0.31 e$, $-0.39 e$, $-0.35 e$, $-0.33 e$, $-0.39 e$, $-0.35 e$ and $-$
158 $0.33e$, respectively, indicating that all RCs are charge-transfer complexes. Similar charge-transfer complexes were also found
159 in our previous study of the $\cdot\text{Cl}$ + piperazine reaction (Ma et al., 2018a).

160 With the master equation theory, the overall rate constants (k_{OH} and k_{Cl}) and branching ratios (Γ) of the $\cdot\text{OH}/\cdot\text{Cl}$ + indole
161 reactions were calculated at 298 K and 1 atm. The calculated k_{OH} and k_{Cl} values of indole are $7.9 \times 10^{-11} \text{ cm}^3 \text{ molecule}^{-1} \text{ s}^{-1}$ and
162 $2.9 \times 10^{-10} \text{ cm}^3 \text{ molecule}^{-1} \text{ s}^{-1}$, respectively. The calculated k_{OH} value is close to the available experimental value of 1.5×10^{-10}
163 $\text{ cm}^3 \text{ molecule}^{-1} \text{ s}^{-1}$ (Atkinson et al., 1995), supporting the reliability of employed computational methods. Over the temperature
164 range 230-330 K (Ma et al., 2018b), the calculated k_{OH} and k_{Cl} values have a negative correlation with temperature (Figure S1).
165 Based on the calculated Γ values of the $\cdot\text{OH}/\cdot\text{Cl}$ + indole reactions (Table 1), it can be concluded that IM₁₋₇ (77%) is the main
166 product for $\cdot\text{OH}$ + indole reaction, and IM₂₋₅ (31%), IM₂₋₆ (46%) and P₂₋₁₀ (C₈H₆N radicals + HCl) (23%) are the main products
167 for $\cdot\text{Cl}$ + indole reaction. In addition, the calculated Γ values of IM₁₋₇, IM₂₋₅, IM₂₋₆ and P₂₋₁₀ (C₈H₆N radicals + HCl) change
168 negligibly with temperature in the range of 230-330 K (Figure S2). Therefore, we mainly considered the further transformation
169 of IM₁₋₇, IM₂₋₅, IM₂₋₆ and C₈H₆N radicals in the following part.

170 **Table 1. Calculated branching ratios (Γ) for the indole + $\cdot\text{OH}/\cdot\text{Cl}$ reactions at 1 atm and 298 K.**

Pathways	Species	Γ	Species	Γ	Species	Γ
$\cdot\text{OH}$ + Indole	IM ₁₋₂	0	IM ₁₋₃	0	IM ₁₋₄	5%
	IM ₁₋₅	12%	IM ₁₋₆	3%	IM ₁₋₇	77%
	IM ₁₋₈	1%	IM ₁₋₉	1%	P ₁₋₁₀	1%
	P ₁₋₁₁	0	P ₁₋₁₂	0	P ₁₋₁₃	0
	P ₁₋₁₄	0	P ₁₋₁₅	0	P ₁₋₁₆	0
$\cdot\text{Cl}$ + Indole	IM ₂₋₅	31%	IM ₂₋₆	46%	P ₂₋₁₀	23%
	P ₂₋₁₁	0	P ₂₋₁₂	0	P ₂₋₁₃	0
	P ₂₋₁₄	0	P ₂₋₁₅	0	P ₂₋₁₆	0

171 3.2 Subsequent Reactions of Addition Intermediates

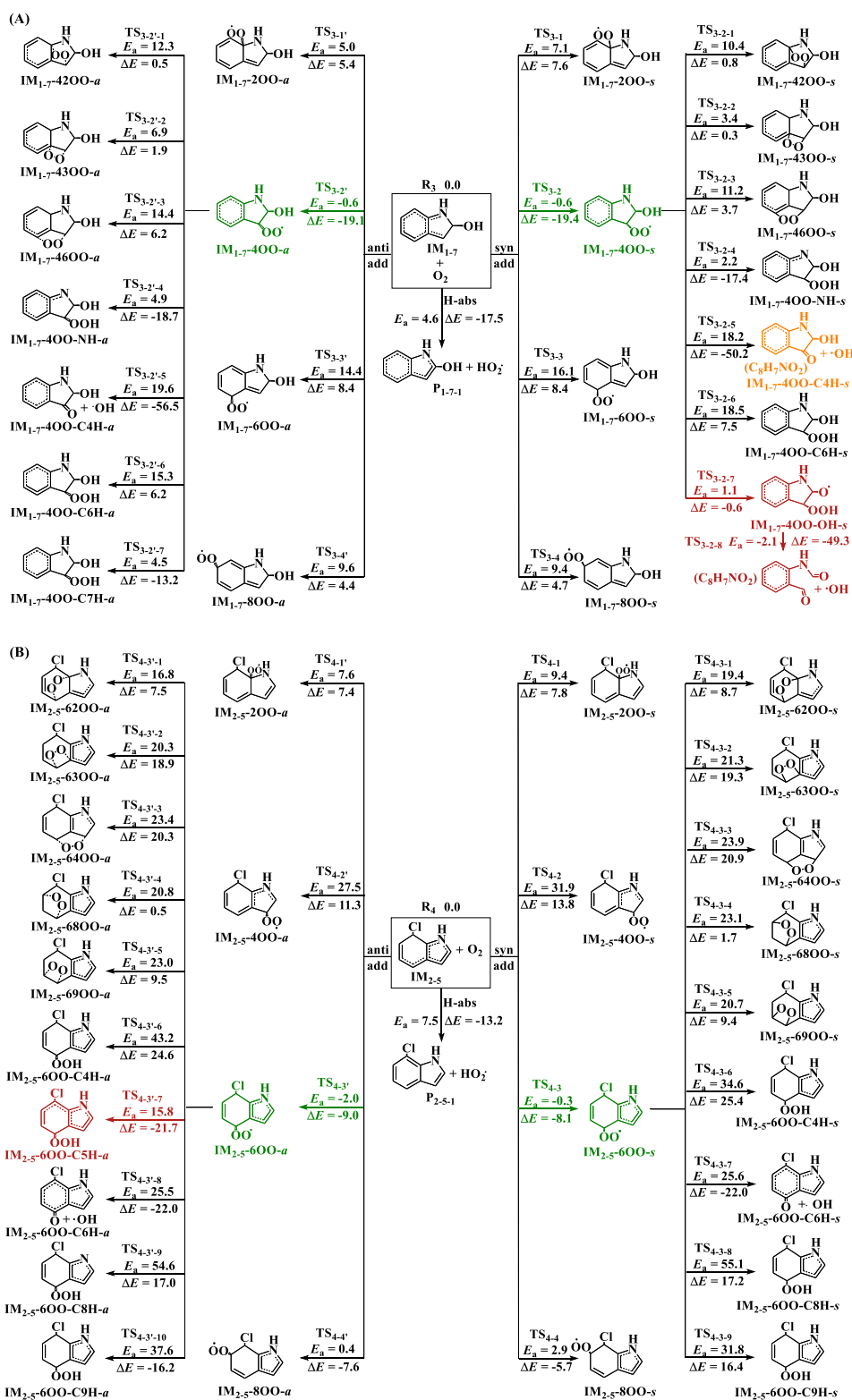
172 Similar to other C-centered radicals (Zhang et al., 2012; Guo et al., 2020; Ma et al., 2021b; Yu et al., 2016; Yu et al., 2017;
173 Ji et al., 2017; Ding et al., 2020a), the intermediates IM₁₋₇, IM₂₋₅ and IM₂₋₆ will subsequently react with O₂. Two different
174 pathways (see Figure 2) were considered for the reactions of the intermediates IM₁₋₇, IM₂₋₅ and IM₂₋₆ with O₂. One is the direct



175 hydrogen abstraction by O_2 from the C site connecting to the -OH or -Cl group forming P_{1-7-1} ($C_8H_7NO + HO_2\cdot$), P_{2-5-1} (C_8H_6NCl
176 + $HO_2\cdot$) and P_{2-6-1} ($C_8H_6NCl + HO_2\cdot$). The other is the O_2 addition to the C sites with high spin density (see spin density
177 distribution in Table S4) of the intermediates IM_{1-7} , IM_{2-5} and IM_{2-6} to form peroxy radicals $Q-iOO-a/s$, where Q stands for
178 intermediates IM_{1-7} , IM_{2-5} and IM_{2-6} , i stands for the numbering of the C-positions where O_2 is added. The O_2 molecule can be
179 added to the same (-syn, abbreviated as -s) and opposite (-anti, abbreviated as -a) sides of the plane relative to -OH or -Cl
180 group. The C2, C4, C6 and C8 sites of IM_{1-7} , C2, C4, C6 and C8 sites of IM_{2-5} and C3, C5, C7 and C9 sites of IM_{2-6} are high
181 spin density sites susceptible for O_2 addition.

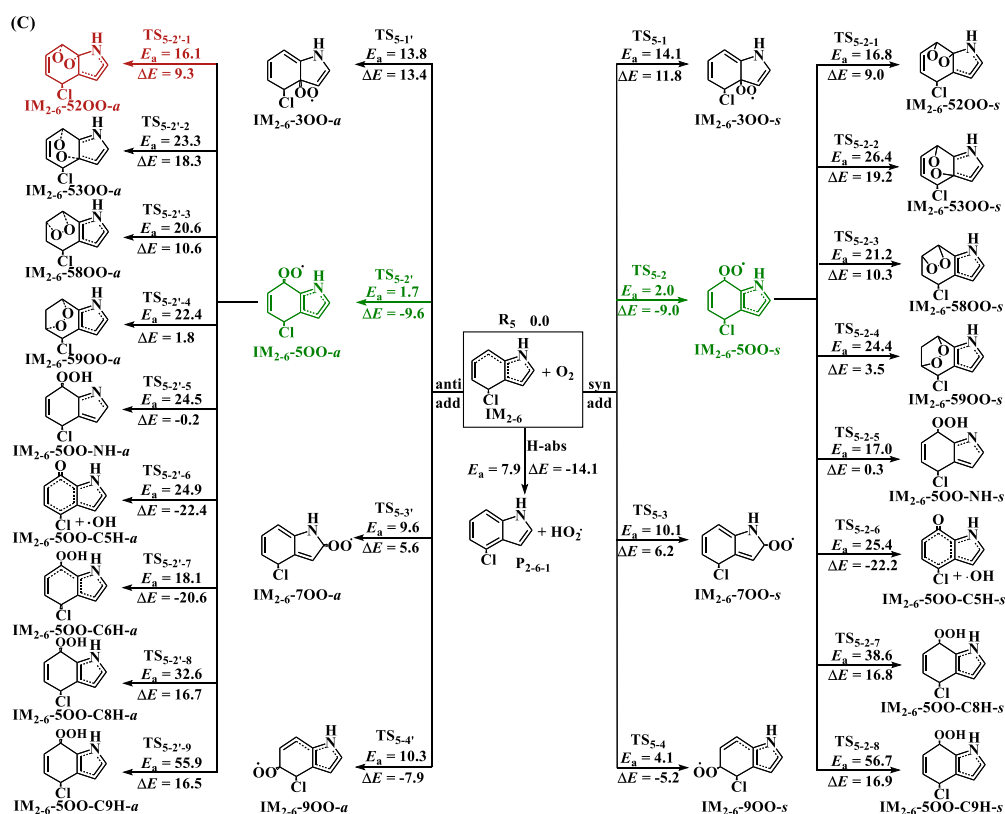
182 As can be seen from the energetic data shown in Figure 2, O_2 addition to the C4 site of IM_{1-7} to form $IM_{1-7-4OO-a/s}$ (-
183 0.6/-0.6 kcal mol⁻¹), C6 site of IM_{2-5} to form $IM_{2-5-6OO-a/s}$ (-0.3/-2.0 kcal mol⁻¹) and C5 site of IM_{2-6} to form $IM_{2-6-5OO-a/s}$
184 (2.0/1.7 kcal mol⁻¹) are the most favorable among all possible entrance pathways for the respective reactions. It deserves
185 mentioning that the formation energy (ΔE) of $IM_{2-5-6OO-a/s}$ and $IM_{2-6-5OO-a/s}$ are only about 9.0 kcal mol⁻¹, which could
186 indicate that they likely re-dissociate back to the reactants IM_{2-5}/IM_{2-6} and O_2 , if $IM_{2-5-6OO-a/s}$ and $IM_{2-6-5OO-a/s}$ does not
187 rapidly transform to other species.

188 For the further transformation of the formed peroxy radicals $IM_{1-7-4OO(-a/s)}$, $IM_{2-5-6OO(-a/s)}$ and $IM_{2-6-5OO(-a/s)}$, two
189 transformation pathways were identified. The first is cyclization reactions where the terminal O-atom of -OO attacks the
190 different C-positions to form bicycle radicals $Q-ijOO(-a/s)$ (j stands the number of the C-positions attacked by terminal O-
191 atom). The second is H-shifts from -OH, -NH- and different -CH- sites to the terminal O-atom to form various hydroperoxide
192 radicals $Q-iOO-OH(-a/s)$, $Q-iOO-NH(-a/s)$ and $Q-iOO-CkH(-a/s)$ (k stands the number of the C-positions from which H is
193 shifted), respectively. For $IM_{1-7-4OO(-a/s)}$ and $IM_{2-5-6OO(-a/s)}$, forming $IM_{1-7-4OO-OH-s}$ and $IM_{2-5-6OO-C5H-a}$ via H-shift
194 reactions are the most favorable, respectively. However, for $IM_{2-6-5OO(-a/s)}$, the cyclization reaction forming $IM_{2-6-52OO-a}$
195 is the most favorable. It is noted that the formed $IM_{1-7-4OO-OH-s}$ from $IM_{1-7-4OO(-a/s)}$ can barrierlessly transform to form
196 $C_8H_7NO_2$ (N-(2-formylphenyl)formamide) and $\cdot OH$ (collectively denoted $P_{1-7-4-1}$) via concerted C-C and O-O bonds rupture.
197 The further transformation of the peroxy radicals $IM_{1-7-4OO(-a/s)}$, $IM_{2-5-6OO(-a/s)}$ and $IM_{2-6-5OO(-a/s)}$ need to overcome
198 barriers above 20.5 kcal mol⁻¹ (relative to their respective peroxy radicals), indicating that the further transformation of IM_{1-7-}
199 $4OO(-a/s)$, $IM_{2-5-6OO(-a/s)}$ and $IM_{2-6-5OO(-a/s)}$ should be very slow.





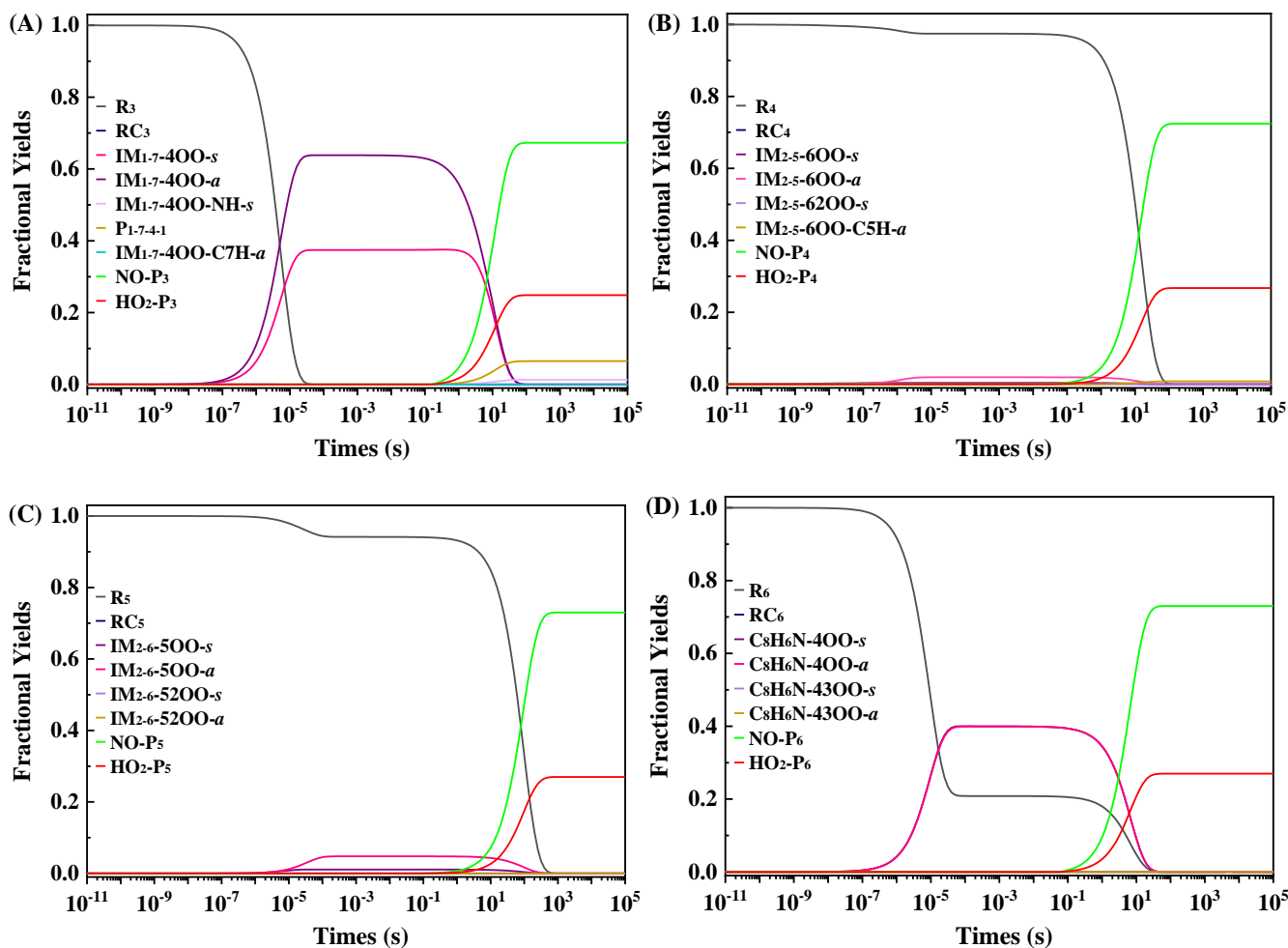
201



202

203 **Figure 2: Reaction pathways and corresponding energetic data for the reactions of IM_{1-7} (A), IM_{2-5} (B) and IM_{2-6} (C)**
 204 **with O_2 . Units are in kcal mol^{-1} .**

205 Based on the energetic data of the favorable reaction pathways, MESMER modeling was employed to investigate the
 206 reaction rate constants and fractional yields for the reactions of IM_{1-7} , IM_{2-5} , and IM_{2-6} with O_2 . Similar to previous studies
 207 (Guo et al., 2020; Ma et al., 2021a; Ma et al., 2021b; Zhang et al., 2012; Fu et al., 2020), bimolecular reactions with NO/HO_2
 208 are considered as competitive pathways for the unimolecular reactions of the peroxy radicals $IM_{1-7-4OO(-a/s)}$, $IM_{2-5-6OO(-a/s)}$
 209 and $IM_{2-6-5OO(-a/s)}$ by simply adding their pseudo-first-order rate constants into the master equation modeling. Here,
 210 applied pseudo first order rate constants for peroxy radicals ($IM_{1-7-4OO(-a/s)}$, $IM_{2-5-6OO(-a/s)}$ and $IM_{2-6-5OO(-a/s)}$) reaction
 211 with NO and HO_2 are 0.06 s^{-1} and 0.02 s^{-1} , respectively, corresponding to reactions occurring at 200 ppt NO and 50 ppt
 212 HO_2 conditions (Hofzumahaus et al., 2009; Yu et al., 2020; Praske et al., 2018). The reactions of peroxy radicals with NO and
 213 HO_2 should form organonitrate/alkoxy radicals (collectively denoted $NO-P_n$, where n marks products from the different
 214 peroxy radical reactions) and hydroperoxide (HO_2-P_n), respectively. Pseudo-first-order rate constants of IM_{1-7} , IM_{2-5} , and IM_{2-6}
 215 with O_2 are calculated to be $3.0 \times 10^7 \text{ s}^{-1}$, based on the reaction rate constants of IM_{1-7} , IM_{2-5} , and IM_{2-6} with O_2 (6.0×10^{-12}
 216 $\text{cm}^3 \text{ molecule}^{-1} \text{ s}^{-1}$) and the concentration of O_2 ($[O_2] = 5.0 \times 10^{18} \text{ molecule cm}^{-3}$). The simulated time-dependent fractional
 217 yields are presented in Figure 3.



218

219

220 **Figure 3: Calculated fractional yields of species (at 200 ppt NO and 50 ppt HO₂· conditions) as a function of time in the**
221 **reactions of IM₁₋₇ (A), IM₂₋₅ (B), IM₂₋₆ (C) and C₈H₆N (D) with O₂ at 298 K and 760 Torr.**

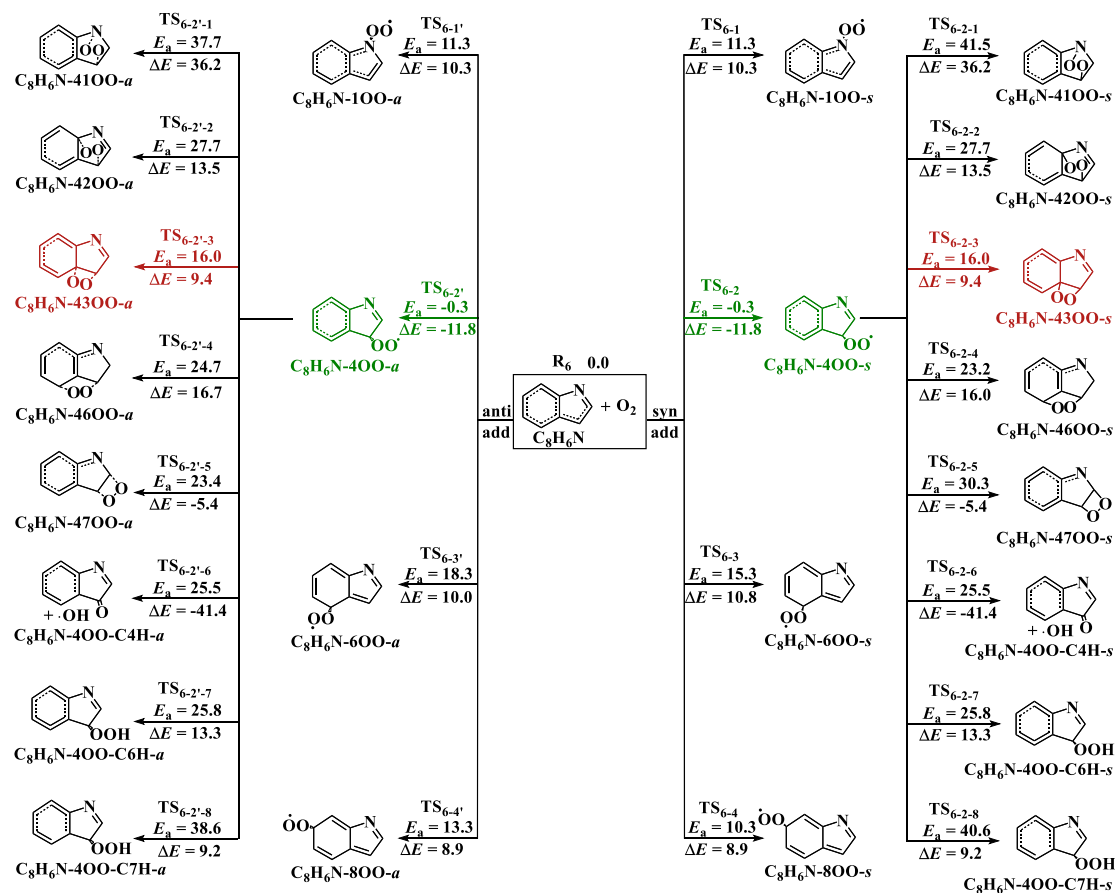
222 As can be seen in Figure 3, after 100 s, the reactions of IM₁₋₇, IM₂₋₅ and IM₂₋₆ with O₂ mainly form the organonitrate/alkoxy
223 radicals NO-P₃ (C₈H₈N₂O₃/C₈H₈NO₂·), NO-P₄ (C₈H₇N₂O₃Cl/C₈H₇NCIO·) and NO-P₅ (C₈H₇N₂O₃Cl/C₈H₇NCIO·), followed by
224 the formation of hydroperoxide HO₂-P₃ (C₈H₉NO₃), HO₂-P₄ (C₈H₈NO₂Cl) and HO₂-P₅ (C₈H₈NO₂Cl), respectively. For the
225 reactions of IM₂₋₅ and IM₂₋₆ with O₂, the main products formed are NO-P_{4/5} and HO₂-P_{4/5}. In contrast, the IM₁₋₇ + O₂ reaction
226 also lead to the fragmental products P₁₋₇₋₄₊₁ (C₈H₇NO₂ and ·OH) besides the main products NO-P₃ and HO₂-P₃. This difference
227 in product branching ratios results from the lower unimolecular reaction energy barrier of the peroxy radicals IM₁₋₇-4OO(-a/s)
228 from the reaction of IM₁₋₇ with O₂ than those of IM₂₋₅-6OO(-a/s) and IM₂₋₆-5OO(-a/s) from the reactions of IM₂₋₅ and IM₂₋₆
229 with O₂. It should be noted that the C₈H₇NO₂ product has been detected in previous experimental study of the ·OH + indole
230 reaction (Montoya-Aguilera et al., 2017), supporting the validity of our computational results.



231 An obvious difference for these three reactions is that the reaction of IM_{1-7} with O_2 can form peroxy radicals $IM_{1-7-4OO}(-$
232 $a/s)$ with high yields during the reactions. However, the yields of the corresponding peroxy radicals $IM_{2-5-6OO}(-a/s)$ and IM_{2-}
233 $6-5OO}(-a/s)$ from the reactions of IM_{2-5} and IM_{2-6} with O_2 are low. The difference mainly originates from the difference in the
234 formation energy of these three peroxy radicals as shown in Figure 2. The ΔE values of $IM_{1-7-4OO}(-a/s)$ (-19.1/-19.4 kcal mol⁻¹)
235 ¹) are much more lower than those of $IM_{2-5-6OO}(-a/s)$ (-9.0/-8.1 kcal mol⁻¹) and $IM_{2-6-5OO}(-a/s)$ (-9.6/-9.0 kcal mol⁻¹). As
236 discussed above, the high formation energy of $IM_{2-5-6OO}(-a/s)$ and $IM_{2-6-5OO}(-a/s)$ should make $IM_{2-5-6OO}(-a/s)$ and IM_{2-6-}
237 $5OO}(-a/s)$ return back to the reactants, explaining the reason for the lower yields of $IM_{2-5-6OO}(-a/s)$ and $IM_{2-6-5OO}(-a/s)$.

238 3.3 Subsequent Reactions of C_8H_6N radicals from the H-abstraction pathway

239 Here, the bimolecular reaction with O_2 was mainly considered for C_8H_6N radicals as its sole atmospheric fate. It was
240 found that the spin density distribution was mainly centered at the C atoms (C4 (0.662), C6 (0.261), C8 (0.178)) and N atom
241 (0.256), indicating that the C_8H_6N radical is delocalized. This is in contrast to previously studied N-centered radicals formed
242 from alkylamines oxidation, which are highly localized (Xie et al., 2015; Xie et al., 2014; Ma et al., 2018a; Tan et al., 2021;
243 Borduas et al., 2015). Therefore, O_2 addition to the C4, C6, C8 and N1 sites (including attack from both sides) are considered
244 for the reaction of the C_8H_6N radicals with O_2 . As can be seen from Figure 4, O_2 additions to the C4 site of the C_8H_6N radicals
245 forming $C_8H_6N-4OO-a/s$ with E_a of -0.3 kcal mol⁻¹ are the most favorable, translating to pseudo-first-order reaction rate
246 constants of 3.0×10^7 s⁻¹. Such rate constants are about 7 orders of magnitude higher than that of typical N-centered radicals
247 reacting with NO even under very high NO concentration (5 ppb). Therefore, C_8H_6N radicals does not react with NO to form
248 carcinogenic nitrosamines in any appreciable amount, which is different from the previously reported reaction mechanism of
249 N-centered radicals formed from the reactions of alkylamines with $\cdot Cl$ (Xie et al., 2015; Xie et al., 2014; Ma et al., 2018a). To
250 the best of our knowledge, this is the first study to reveal despite forming radicals by abstracting an H-atom at the N-site,
251 carcinogenic nitrosamines were not produced in the indole oxidation reaction.



252

253 **Figure 4: Reaction pathways and corresponding energetic data for the reactions of C_8H_6N radicals with O_2 . Units are**
 254 **in kcal mol⁻¹.**

255 For the transformation of the formed $C_8H_6N-400-a/s$ radicals, the ring closure reaction to form $C_8H_6N-4300-a/s$ is the
 256 most favorable, but still needs to overcome a 27.8 kcal mol⁻¹ energy barrier, therefore the further transformation of the formed
 257 $C_8H_6N-400-a/s$ should proceed very slowly. The $C_8H_6N-400-a/s$ should mainly react with NO and $HO_2\cdot$ to form NO-P₆ and
 258 HO_2 -P₆. Detailed kinetics calculations (Figure 3D) further confirm that the reaction of C_8H_6N radicals with O_2 mainly form
 259 NO-P₆ and HO_2 -P₆ under 200 ppt NO and 50 ppt $HO_2\cdot$ conditions.

260 4 Comparison with Available Experimental Results and Atmospheric Implications.

261 This study found that $\cdot OH/\cdot Cl$ initiated reactions of indole mainly form organonitrates, alkoxy radicals and hydroperoxide
 262 products with N-(2-formylphenyl)formamide ($C_8H_7NO_2$) as a minor product at 200 ppt NO and 50 ppt $HO_2\cdot$ conditions. The
 263 formed closed-shell products have high oxygen-to-carbon ratios compared to indole and therefore are expected to have lower
 264 vapor pressures, likely being first generation products that can be further oxidized and contribute to the formation of SOA.



265 With our findings, a comparison was made with the available experimental study on $\cdot\text{OH}$ initiated reaction of indole. The
266 calculated k_{OH} values ($7.9 \times 10^{-11} \text{ cm}^3 \text{ molecule}^{-1} \text{ s}^{-1}$) of indole is consistent with the experimental value ($15 \times 10^{-11} \text{ cm}^3$
267 $\text{molecule}^{-1} \text{ s}^{-1}$) (Atkinson et al., 1995), indicating the reliability of applied theoretical methods. A signal with the molecular
268 formula $\text{C}_8\text{H}_7\text{NO}_2$ has been observed in the mass spectrum in an experimental study (Montoya-Aguilera et al., 2017),
269 supporting the formation of the predicted N-(2-formylphenyl)formamide. To the best of our knowledge, this study is the first
270 to reveal the chemical identity of the mass spectrum signal as N-(2-formylphenyl)formamide, as opposed to the proposed 3-
271 oxy-2-hydroxy-indole. In addition, monomeric products (isatin and isatoic anhydride) and dimer products has not been
272 observed in our computational study. We speculate that they may be produced from the subsequent conversion of the formed
273 alkoxy radicals, multi-generation reactions of organonitrates and hydroperoxide and cross reactions of peroxy radicals ($\text{RO}_2 +$
274 RO_2). Therefore, further studies are warranted to investigate the subsequent transformation of the formed alkoxy radicals,
275 organonitrates and hydroperoxide, and the $\text{RO}_2 + \text{RO}_2$ reactions, to accurately describe the atmospheric impact of indole.

276 The calculated k_{Cl} value of the indole + $\cdot\text{Cl}$ reaction is a factor of 3.7 higher than that of the indole + $\cdot\text{OH}$ reaction, and is
277 close to the k_{Cl} values for the reactions of alkylamines, heterocyclic amines and amides with $\cdot\text{Cl}$ (Xie et al., 2017; Xie et al.,
278 2015; Ma et al., 2018a; Nicovich et al., 2015). The contribution of $\cdot\text{Cl}$ to the transformation of indole is calculated to be 3.6-
279 36% that of $\cdot\text{OH}$, assuming $\cdot\text{Cl}$ concentrations equal to 1-10% of that of $\cdot\text{OH}$ (Wang and Ruiz, 2017; Nicovich et al., 2015;
280 Xie et al., 2017; Xie et al., 2015; Ma et al., 2018a). Therefore, $\cdot\text{Cl}$ plays an important role in the overall transformation of
281 indole. More importantly, $\cdot\text{Cl}$ initiated reaction of indole does not lead to the formation of carcinogenic nitrosamines although
282 $\cdot\text{Cl}$ can favorably abstract the H-atom from N-site to form $\text{C}_8\text{H}_6\text{N}$ radicals, which is a plausible precursor of carcinogenic
283 nitrosamines. Hence, to the best of our knowledge, this is the first study to reveal despite forming radicals by abstracting an
284 H-atom at the N-site, carcinogenic nitrosamines were not produced in the indole oxidation reaction. This is most likely caused
285 by the delocalized character of the formed $\text{C}_8\text{H}_6\text{N}$ radicals due to the existence of the adjacent unsaturated bonds. Therefore,
286 this study further confirm that the functional groups connected to the NH_x ($x = 1, 2$) group highly affect the atmospheric fate
287 of ONCs. Further studies should be performed to investigate the structure-activity relationship of $\cdot\text{Cl}$ initiated reactions of
288 ONCs to comprehensively evaluate their atmospheric impacts.

289

290 *Data availability.* The data in this article are available from the corresponding author upon request (maff@dlut.edu.cn,
291 hbxie@dlut.edu.cn).

292 *Author contribution.* FFM and HBX designed research; JWX, FFM and HBX performed research; JWX, FFM and HBX
293 analyzed data; JWX, FFM, HBX and JWC wrote the paper; and FFM, HBX and JWC reviewed and revised the paper.

294 *Competing interests.* The authors declare that they have no conflict of interest.



295 *Acknowledgements.* The study was supported by the LiaoNing Revitalization Talents Program (XLYC1907194), National
296 Natural Science Foundation of China (21876024), the Major International (Regional) Joint Research Project (21661142001)
297 and Supercomputing Center of Dalian University of Technology.

298 **References**

- 299 Almeida, J., Schobesberger, S., Kürten, A., Ortega, I. K., Kupiainen-Määttä, O., Praplan, A. P., Adamov, A., Amorim, A.,
300 Bianchi, F., Breitenlechner, M., David, A., Dommen, J., Donahue, N. M., Downard, A., Dunne, E., Duplissy, J., Ehrhart, S.,
301 Flagan, R. C., Franchin, A., Guida, R., Hakala, J., Hansel, A., Heinritzi, M., Henschel, H., Jokinen, T., Junninen, H., Kajos,
302 M., Kangasluoma, J., Keskinen, H., Kupc, A., Kurtén, T., Kvashin, A. N., Laaksonen, A., Lehtipalo, K., Leiminger, M., Leppä,
303 J., Loukonen, V., Makhmutov, V., Mathot, S., McGrath, M. J., Nieminen, T., Olenius, T., Onnela, A., Petäjä, T., Riccobono,
304 F., Riipinen, I., Rissanen, M., Rondo, L., Ruuskanen, T., Santos, F. D., Sarnela, N., Schallhart, S., Schnitzhofer, R., Seinfeld,
305 J. H., Simon, M., Sipilä, M., Stozhkov, Y., Stratmann, F., Tomé, A., Tröstl, J., Tsagkogeorgas, G., Vaattovaara, P., Viisanen,
306 Y., Virtanen, A., Vrtala, A., Wagner, P. E., Weingartner, E., Wex, H., Williamson, C., Wimmer, D., Ye, P., Yli-Juuti, T.,
307 Carslaw, K. S., Kulmala, M., Curtius, J., Baltensperger, U., Worsnop, D. R., Vehkamäki, H., and Kirkby, J.: Molecular
308 understanding of sulphuric acid-amine particle nucleation in the atmosphere, *Nature*, 502, 359-363,
309 <https://doi.org/10.1038/nature12663>, 2013.
- 310 Atkinson, R., Tuazon, E. C., Arey, J., and Aschmann, S. M.: Atmospheric and indoor chemistry of gas-phase indole, quinoline,
311 and isoquinoline, *Atmos. Environ.*, 29, 3423-3432, [https://doi.org/10.1016/1352-2310\(95\)00103-6](https://doi.org/10.1016/1352-2310(95)00103-6), 1995.
- 312 Atkinson, R., Baulch, D. L., Cox, R. A., Hampson, R. F., Kerr, J. A., and Troe, J.: Evaluated Kinetic and Photochemical Data
313 for Atmospheric Chemistry: Supplement III. IUPAC Subcommittee on Gas Kinetic Data Evaluation for Atmospheric
314 Chemistry, *J. Phys. Chem. Ref. Data*, 18, 881-1097, <https://doi.org/10.1063/1.555832>, 1989.
- 315 Barker, J. R.: Multiple-well, multiple-path unimolecular reaction systems. I. MultiWell computer program suite, *Int. J. Chem.*
316 *Kinet.*, 33, 232-245, <https://doi.org/10.1002/kin.1017>, 2001.
- 317 Barker, J. R. and Ortiz, N. F.: Multiple-Well, multiple-path unimolecular reaction systems. II. 2-methylhexyl free radicals, *Int.*
318 *J. Chem. Kinet.*, 33, 246-261, <https://doi.org/10.1002/kin.1018>, 2001.
- 319 Borduas, N., da Silva, G., Murphy, J. G., and Abbatt, J. P. D.: Experimental and Theoretical Understanding of the Gas Phase
320 Oxidation of Atmospheric Amides with OH Radicals: Kinetics, Products, and Mechanisms, *J. Phys. Chem. A*, 119, 4298-4308,
321 <https://doi.org/10.1021/jp503759f>, 2015.
- 322 Borduas, N., Abbatt, J. P. D., Murphy, J. G., So, S., and da Silva, G.: Gas-Phase Mechanisms of the Reactions of Reduced
323 Organic Nitrogen Compounds with OH Radicals, *Environ. Sci. Technol.*, 50, 11723-11734,
324 <https://doi.org/10.1021/acs.est.6b03797>, 2016.



- 325 Borduas, N., Murphy, J. G., Wang, C., da Silva, G., and Abbatt, J. P. D.: Gas Phase Oxidation of Nicotine by OH Radicals:
326 Kinetics, Mechanisms, and Formation of HNCO, *Environ. Sci. Technol. Lett.*, **3**, 327-331,
327 <https://doi.org/10.1021/acs.estlett.6b00231>, 2016.
- 328 Bunkan, A. J. C., Mikoviny, T., Nielsen, C. J., Wisthaler, A., and Zhu, L.: Experimental and Theoretical Study of the OH-
329 Initiated Photo-oxidation of Formamide, *J. Phys. Chem. A*, **120**, 1222-1230, <https://doi.org/10.1021/acs.jpca.6b00032>, 2016.
- 330 Bunkan, A. J. C., Hetzler, J., Mikoviny, T., Wisthaler, A., Nielsen, C. J., and Olzmann, M.: The reactions of N-
331 methylformamide and N,N-dimethylformamide with OH and their photo-oxidation under atmospheric conditions:
332 experimental and theoretical studies, *Phys. Chem. Chem. Phys.*, **17**, 7046-7059, <https://doi.org/10.1039/C4CP05805D>, 2015.
- 333 Cardoza, Y. J., Lait, C. G., Schmelz, E. A., Huang, J., and Tumlinson, J. H.: Fungus-Induced Biochemical Changes in Peanut
334 Plants and Their Effect on Development of Beet Armyworm, *Spodoptera Exigua* Hübner (Lepidoptera: Noctuidae) Larvae,
335 *Environ. Entomol.*, **32**, 220-228, <https://doi.org/10.1603/0046-225X-32.1.220>, 2003.
- 336 Chen, J., Jiang, S., Liu, Y.-R., Huang, T., Wang, C. Y., Miao, S. K., Wang, Z. Q., Zhang, Y., and Huang, W.: Interaction of
337 oxalic acid with dimethylamine and its atmospheric implications, *RSC Adv.*, **7**, 6374-6388,
338 <https://doi.org/10.1039/C6RA27945G>, 2017.
- 339 Crouse, J. D., Nielsen, L. B., Jørgensen, S., Kjaergaard, H. G., and Wennberg, P. O.: Autoxidation of Organic Compounds
340 in the Atmosphere, *J. Phys. Chem. Lett.*, **4**, 3513-3520, <https://doi.org/10.1021/jz4019207>, 2013.
- 341 Ding, Z., Yi, Y., Wang, W., and Zhang, Q.: Atmospheric oxidation of indene initiated by OH radical in the presence of O₂ and
342 NO: A mechanistic and kinetic study, *Chemosphere*, **259**, 127331, <https://doi.org/10.1016/j.chemosphere.2020.127331>, 2020a.
- 343 Ding, Z., Yi, Y., Wang, W., and Zhang, Q.: Understanding the role of Cl and NO₃ radicals in initiating atmospheric oxidation
344 of fluorene: A mechanistic and kinetic study, *Sci. Total Environ.*, **716**, 136905,
345 <https://doi.org/10.1016/j.scitotenv.2020.136905>, 2020b.
- 346 da Silva, G.: Formation of Nitrosamines and Alkyldiazohydroxides in the Gas Phase: The CH₃NH + NO Reaction Revisited,
347 *Environ. Sci. Technol.*, **47**, 7766-7772, <https://doi.org/10.1021/es401591n>, 2013.
- 348 Eckart, C.: The penetration of a potential barrier by electrons, *Phys. Rev.*, **35**, 1303-1309,
349 <https://doi.org/10.1103/PhysRev.35.1303>, 1930.
- 350 Ehn, M., Thornton, J. A., Kleist, E., Sipilä, M., Junninen, H., Pullinen, I., Springer, M., Rubach, F., Tillmann, R., Lee, B.,
351 Lopez-Hilfiker, F., Andres, S., Acir, I.-H., Rissanen, M., Jokinen, T., Schobesberger, S., Kangasluoma, J., Kontkanen, J.,
352 Nieminen, T., Kurtén, T., Nielsen, L. B., Jørgensen, S., Kjaergaard, H. G., Canagaratna, M., Maso, M. D., Berndt, T., Petäjä,
353 T., Wahner, A., Kerminen, V.-M., Kulmala, M., Worsnop, D. R., Wildt, J., and Mentel, T. F.: A large source of low-volatility
354 secondary organic aerosol, *Nature*, **506**, 476-479, <https://doi.org/10.1038/nature13032>, 2014.
- 355 Faxon, C. B. and Allen, D. T.: Chlorine chemistry in urban atmospheres: a review, *Environ. Chem.*, **10**, 221-233,
356 <https://doi.org/10.1071/en13026>, 2013.



- 357 Fu, Z., Xie, H. B., Elm, J., Guo, X., Fu, Z., and Chen, J.: Formation of Low-Volatile Products and Unexpected High
358 Formaldehyde Yield from the Atmospheric Oxidation of Methylsiloxanes, *Environ. Sci. Technol.*, 54, 7136-7145,
359 <https://doi.org/10.1021/acs.est.0c01090>, 2020.
- 360 Frisch, M. J., Trucks, G. W., Schlegel, H. B., Scuseria, G. E., Robb, M. A., Cheeseman, J. R., Scalmani, G., Barone, V.,
361 Mennucci, B., Petersson, G. A., Nakatsuji, H., Caricato, M., Li, X., Hratchian, H. P., Izmaylov, A. F., Bloino, J., Zheng, G.,
362 Sonnenberg, J. L., Hada, M., Ehara, M., Toyota, K., Fukuda, R., Hasegawa, J., Ishida, M., Nakajima, T., Honda, Y., Kitao, O.,
363 Nakai, H., Vreven, T., Montgomery, J. A., Jr, Peralta, J. E., Ogliaro, F., Bearpark, M., Heyd, J. J., Brothers, E., Kudin, K. N.,
364 Staroverov, V. N., Kobayashi, R., Normand, J., Raghavachari, K., Rendell, A., Burant, J. C., Iyengar, S. S., Tomasi, J., Cossi,
365 M., Rega, N., Millam, J. M., Klene, M., Knox, J. E., Cross, J. B., Bakken, V., Adamo, C., Jaramillo, J., Gomperts, R., Stratmann,
366 R. E., Yazyev, O., Austin, A. J., Cammi, R., Pomelli, C., Ochterski, J. W., Martin, R. L., Morokuma, K., Zakrzewski, V. G.,
367 Voth, G. A., Salvador, P., Dannenberg, J. J., Dapprich, S., Daniels, A. D., Farkas, O., Foresman, J. B., Ortiz, J. V., Cioslowski,
368 J., and Fox, D. J.: *Gaussian 09*, Gaussian Inc., 2009.
- 369 Ge, X., Wexler, A. S., and Clegg, S. L.: Atmospheric amines – Part I. A review, *Atmos. Environ.*, 45, 524-546,
370 <https://doi.org/10.1016/j.atmosenv.2010.10.012>, 2011.
- 371 Gentner, D. R., Ormeño, E., Fares, S., Ford, T. B., Weber, R., Park, J. H., Brioude, J., Angevine, W. M., Karlik, J. F., and
372 Goldstein, A. H.: Emissions of terpenoids, benzenoids, and other biogenic gas-phase organic compounds from agricultural
373 crops and their potential implications for air quality, *Atmos. Chem. Phys.*, 14, 5393-5413, [https://doi.org/10.5194/acp-14-](https://doi.org/10.5194/acp-14-5393-2014)
374 [5393-2014](https://doi.org/10.5194/acp-14-5393-2014), 2014.
- 375 Glowacki, D. R., Liang, C.-H., Morley, C., Pilling, M. J., and Robertson, S. H.: MESMER: An Open-Source Master Equation
376 Solver for Multi-Energy Well Reactions, *J. Phys. Chem. A*, 116, 9545-9560, <https://doi.org/10.1021/jp3051033>, 2012.
- 377 Guo, X., Ma, F., Liu, C., Niu, J., He, N., Chen, J., and Xie, H. B.: Atmospheric oxidation mechanism and kinetics of isoprene
378 initiated by chlorine radicals: A computational study, *Sci. Total Environ.*, 712, 136330,
379 <https://doi.org/10.1016/j.scitotenv.2019.136330>, 2020.
- 380 Holbrook, K. A., Pilling, M. J., Robertson, S. H., and Robinson, P. J.: *Unimolecular Reactions*, 2nd ed, Wiley: New York, 1996.
- 381 Jahn, L. G., Wang, D. S., Dhulipala, S. V., Ruiz, L. H. et al. Gas-phase chlorine radical oxidation of alkanes: Effects of
382 structural branching, NO_x, and relative humidity observed during environmental chamber experiments, *The Journal of Physical*
383 *Chemistry A*, 125(33): 7303-7317, <https://doi.org/10.1021/acs.jpca.1c03516>, 2021.
- 384 Ji, Y., Wang, H., Gao, Y., Li, G., and An, T. C.: A theoretical model on the formation mechanism and kinetics of highly toxic
385 air pollutants from halogenated formaldehydes reacted with halogen atoms, *Atmos. Chem. Phys.*, 13, 11277-11286,
386 <https://doi.org/10.5194/acp-13-11277-2013>, 2013.
- 387 Ji, Y., Zheng, J., Qin, D., Li, Y., Gao, Y., Yao, M., Chen, X., Li, G., An, T., and Zhang, R.: OH-Initiated Oxidation of
388 Acetylacetone: Implications for Ozone and Secondary Organic Aerosol Formation, *Environ. Sci. Technol.*, 52, 11169-11177,
389 [10.1021/acs.est.8b03972](https://doi.org/10.1021/acs.est.8b03972), 2018.



- 390 Ji, Y., Zhao, J., Terazono, H., Misawa, K., Levitt, N. P., Li, Y., Lin, Y., Peng, J., Wang, Y., Duan, L., Pan, B., Zhang, F., Feng,
391 X., An, T., Marrero-Ortiz, W., Secrest, J., Zhang, A. L., Shibuya, K., Molina, M. J., and Zhang, R.: Reassessing the atmospheric
392 oxidation mechanism of toluene, *Proc. Natl. Acad. Sci. U.S.A.*, 114, 8169, [10.1073/pnas.1705463114](https://doi.org/10.1073/pnas.1705463114), 2017.
- 393 Karl, T., Striednig, M., Graus, M., Hammerle, A., and Wohlfahrt, G.: Urban flux measurements reveal a large pool of
394 oxygenated volatile organic compound emissions, *Proc. Natl. Acad. Sci. U.S.A.*, 115, 1186,
395 <https://doi.org/10.1073/pnas.1714715115>, 2018.
- 396 Khare, P. and Gentner, D. R.: Considering the future of anthropogenic gas-phase organic compound emissions and the
397 increasing influence of non-combustion sources on urban air quality, *Atmos. Chem. Phys.*, 18, 5391-5413,
398 <https://doi.org/10.5194/acp-18-5391-2018>, 2018.
- 399 Laskin, A., Smith, J. S., and Laskin, J.: Molecular Characterization of Nitrogen-Containing Organic Compounds in Biomass
400 Burning Aerosols Using High-Resolution Mass Spectrometry, *Environ. Sci. Technol.*, 43, 3764-3771,
401 <https://doi.org/10.1021/es803456n>, 2009.
- 402 Le Breton, M., Hallquist, Å. M., Pathak, R. K., Simpson, D., Wang, Y., Johansson, J., Zheng, J., Yang, Y., Shang, D., Wang,
403 H., Liu, Q., Chan, C., Wang, T., Bannan, T. J., Priestley, M., Percival, C. J., Shallcross, D. E., Lu, K., Guo, S., Hu, M., and
404 Hallquist, M.: Chlorine oxidation of VOCs at a semi-rural site in Beijing: significant chlorine liberation from ClNO₂ and
405 subsequent gas- and particle-phase Cl-VOC production, *Atmos. Chem. Phys.*, 18, 13013-13030, [https://doi.org/10.5194/acp-](https://doi.org/10.5194/acp-18-13013-2018)
406 [18-13013-2018](https://doi.org/10.5194/acp-18-13013-2018), 2018.
- 407 Hofzumahaus, A., Rohrer, F., Lu, K., Bohn, B., Brauers, T., Chang, C.-C., Fuchs, H., Holland, F., Kita, K., Kondo, Y., Li, X.,
408 Lou, S., Shao, M., Zeng, L., Wahner, A., and Zhang, Y.: Amplified Trace Gas Removal in the Troposphere, *Science*, 324,
409 1702-1704, <https://doi.org/10.1126/science.1164566>, 2009.
- 410 Lewis Alastair, C.: The changing face of urban air pollution, *Science*, 359, 744-745, <https://doi.org/10.1126/science.aar4925>,
411 2018.
- 412 Li, J., Zhang, N., Wang, P., Choi, M., Ying, Q., Guo, S., Lu, K., Qiu, X., Wang, S., Hu, M., Zhang, Y., and Hu, J.: Impacts of
413 chlorine chemistry and anthropogenic emissions on secondary pollutants in the Yangtze river delta region, *Environ. Pollut.*,
414 287, 117624, <https://doi.org/10.1016/j.envpol.2021.117624>, 2021.
- 415 Li, K., Li, J., Tong, S., Wang, W., Huang, R. J., and Ge, M.: Characteristics of wintertime VOCs in suburban and urban Beijing:
416 concentrations, emission ratios, and festival effects, *Atmos. Chem. Phys.*, 19, 8021-8036, [https://doi.org/10.5194/acp-19-8021-](https://doi.org/10.5194/acp-19-8021-2019)
417 [2019](https://doi.org/10.5194/acp-19-8021-2019), 2019.
- 418 Lin, Y., Ji, Y., Li, Y., Secrest, J., Xu, W., Xu, F., Wang, Y., An, T., and Zhang, R.: Interaction between succinic acid and
419 sulfuric acid-base clusters, *Atmos. Chem. Phys.*, 19, 8003-8019, <https://doi.org/10.5194/acp-19-8003-2019>, 2019.
- 420 Ma, F.F., Xie, H.-B., Li, M., Wang, S., Zhang, R., and Chen, J.: Autoxidation mechanism for atmospheric oxidation of tertiary
421 amines: Implications for secondary organic aerosol formation, *Chemosphere*, 273, 129207,
422 <https://doi.org/10.1016/j.chemosphere.2020.129207>, 2021a.



- 423 Ma, F.F., Xie, H. B., Elm, J., Shen, J., Chen, J., and Vehkamäki, H.: Piperazine Enhancing Sulfuric Acid-Based New Particle
424 Formation: Implications for the Atmospheric Fate of Piperazine, *Environ. Sci. Technol.*, **53**, 8785-8795,
425 <https://doi.org/10.1021/acs.est.9b02117>, 2019.
- 426 Ma, F.F., Guo, X. R., Xia, D. M., Xie, H. B., Wang, Y., Elm, J., Chen, J., and Niu, J.: Atmospheric Chemistry of Allylic
427 Radicals from Isoprene: A Successive Cyclization-Driven Autoxidation Mechanism, *Environ. Sci. Technol.*, **55**, 4399-4409,
428 <https://doi.org/10.1021/acs.est.0c07925>, 2021b.
- 429 Ma, F.F., Ding, Z. Z., Elm, J., Xie, H. B., Yu, Q., Liu, C., Li, C., Fu, Z., Zhang, L., and Chen, J.: Atmospheric Oxidation of
430 Piperazine Initiated by $\cdot\text{Cl}$: Unexpected High Nitrosamine Yield, *Environ. Sci. Technol.*, **52**, 9801-9809,
431 <https://doi.org/10.1021/acs.est.8b02510>, 2018a.
- 432 Ma, F.F., Xie, H. B., and Chen, J.: Benchmarking of DFT functionals for the kinetics and mechanisms of atmospheric addition
433 reactions of OH radicals with phenyl and substituted phenyl-based organic pollutants, *Int. J. Quantum Chem.*, **118**, e25533,
434 <https://doi.org/10.1002/qua.25533>, 2018b.
- 435 Ma, Q., Meng, N., Li, Y., and Wang, J.: Occurrence, impacts, and microbial transformation of 3-methylindole (skatole): A
436 critical review, *J. Hazard. Mater.*, **416**, 126181, <https://doi.org/10.1016/j.jhazmat.2021.126181>, 2021b.
- 437 MacLeod, M., Scheringer, M., Podey, H., Jones, K. C., and Hungerbühler, K.: The Origin and Significance of Short-Term
438 Variability of Semivolatile Contaminants in Air, *Environ. Sci. Technol.*, **41**, 3249-3253, <https://doi.org/10.1021/es062135w>,
439 2007.
- 440 McKee, M. L., Nicolaidis, A., and Radom, L.: A Theoretical Study of Chlorine Atom and Methyl Radical Addition to Nitrogen
441 Bases: Why Do Cl Atoms Form Two-Center-Three-Electron Bonds Whereas CH_3 Radicals Form Two-Center-Two-Electron
442 Bonds, *J. Am. Chem. Soc.*, **118**, 10571-10576, <https://doi.org/10.1021/ja9613973>, 1996.
- 443 Misztal, P. K., Hewitt, C. N., Wildt, J., Blande, J. D., Eller, A. S. D., Fares, S., Gentner, D. R., Gilman, J. B., Graus, M.,
444 Greenberg, J., Guenther, A. B., Hansel, A., Harley, P., Huang, M., Jardine, K., Karl, T., Kaser, L., Keutsch, F. N., Kiendler-
445 Scharr, A., Kleist, E., Lerner, B. M., Li, T., Mak, J., Nölscher, A. C., Schnitzhofer, R., Sinha, V., Thornton, B., Warneke, C.,
446 Wegener, F., Werner, C., Williams, J., Worton, D. R., Yassaa, N., and Goldstein, A. H.: Atmospheric benzenoid emissions
447 from plants rival those from fossil fuels, *Sci. Rep.*, **5**, 12064, <https://doi.org/10.1038/srep12064>, 2015.
- 448 Montgomery, J. A., Frisch, M. J., Ochterski, J. W., and Petersson, G. A.: A complete basis set model chemistry. VI. Use of
449 density functional geometries and frequencies, *J. Chem. Phys.*, **110**, 2822-2827, <https://doi.org/10.1063/1.477924>, 1999.
- 450 Montoya-Aguilera, J., Horne, J. R., Hinks, M. L., Fleming, L. T., Perraud, V., Lin, P., Laskin, A., Laskin, J., Dabdub, D., and
451 Nizkorodov, S. A.: Secondary organic aerosol from atmospheric photooxidation of indole, *Atmos. Chem. Phys.*, **17**, 11605-
452 11621, <https://doi.org/10.5194/acp-17-11605-2017>, 2017.
- 453 Nicovich, J. M., Mazumder, S., Laine, P. L., Wine, P. H., Tang, Y., Bunkan, A. J. C., and Nielsen, C. J.: An experimental and
454 theoretical study of the gas phase kinetics of atomic chlorine reactions with CH_3NH_2 , $(\text{CH}_3)_2\text{NH}$, and $(\text{CH}_3)_3\text{N}$, *Phys. Chem.*
455 *Chem. Phys.*, **17**, 911-917, <https://doi.org/10.1039/C4CP03801K>, 2015.



- 456 Nielsen, C. J., Herrmann, H., and Weller, C.: Atmospheric chemistry and environmental impact of the use of amines in carbon
457 capture and storage (CCS), *Chem. Soc. Rev.*, 41, 6684-6704, <https://doi.org/10.1039/C2CS35059A>, 2012.
- 458 Onel, L., Dryden, M., Blitz, M. A., and Seakins, P. W.: Atmospheric Oxidation of Piperazine by OH has a Low Potential to
459 Form Carcinogenic Compounds, *Environ. Sci. Technol. Lett.*, 1, 367-371, <https://doi.org/10.1021/ez5002159>, 2014a.
- 460 Onel, L., Blitz, M., Dryden, M., Thonger, L., and Seakins, P.: Branching Ratios in Reactions of OH Radicals with Methylamine,
461 Dimethylamine, and Ethylamine, *Environ. Sci. Technol.*, 48, 9935-9942, <https://doi.org/10.1021/es502398r>, 2014b.
- 462 Praske, E., Otkjær, R. V., Crouse, J. D., Hethcox, J. C., Stoltz, B. M., Kjaergaard, H. G., and Wennberg, P. O.: Atmospheric
463 autoxidation is increasingly important in urban and suburban North America, *Proc. Natl. Acad. Sci. U.S.A.*, 115, 64,
464 <https://doi.org/110.1073/pnas.1715540115>, 2018.
- 465 Reed, A. E., Weinstock, R. B., and Weinhold, F.: Natural population analysis, *J. Chem. Phys.*, 83, 735-746,
466 <https://doi.org/10.1063/1.449486>, 1985.
- 467 Ren, Z. and da Silva, G.: Atmospheric Oxidation of Piperazine Initiated by OH: A Theoretical Kinetics Investigation, *ACS*
468 *Earth Space Chem.*, 3, 2510-2516, <https://doi.org/10.1021/acsearthspacechem.9b00227>, 2019.
- 469 Riedel, T. P., Bertram, T. H., Crisp, T. A., Williams, E. J., Lerner, B. M., Vlasenko, A., Li, S.-M., Gilman, J., de Gouw, J.,
470 Bon, D. M., Wagner, N. L., Brown, S. S., and Thornton, J. A.: Nitryl Chloride and Molecular Chlorine in the Coastal Marine
471 Boundary Layer, *Environ. Sci. Technol.*, 46, 10463-10470, <https://doi.org/10.1021/es204632r>, 2012.
- 472 Rienstra-Kiracofe, J. C., Allen, W. D., and Schaefer, H. F.: The $C_2H_5 + O_2$ Reaction Mechanism: High-Level ab Initio
473 Characterizations, *J. Phys. Chem. A*, 104, 9823-9840, <https://doi.org/10.1021/jp001041k>, 2000.
- 474 Robinson, P. J., and Holbrook, K. A.: *Unimolecular Reactions*, John Wiley & Sons: New York, 1972.
- 475 SenGupta, S., Indulkar, Y., Kumar, A., Dhanya, S., Naik, P. D., and Bajaj, P. N.: Kinetics of Gas-Phase Reaction of OH with
476 Morpholine: An Experimental and Theoretical Study, *J. Phys. Chem. A*, 114, 7709-7715, <https://doi.org/10.1021/jp101464x>,
477 2010.
- 478 Schade, G. W. and Crutzen, P. J.: Emission of aliphatic amines from animal husbandry and their reactions: Potential source of
479 N_2O and HCN, *J. Atmos. Chem.*, 22, 319-346, <https://doi.org/10.1007/BF00696641>, 1995.
- 480 Shiels, O. J., Kelly, P. D., Bright, C. C., Poad, B. L. J., Blanksby, S. J., da Silva, G., and Trevitt, A. J.: Reactivity Trends in the
481 Gas-Phase Addition of Acetylene to the N-Protonated Aryl Radical Cations of Pyridine, Aniline, and Benzonitrile, *J. Am. Soc.*
482 *Mass. Spectrom.*, 32, 537-547, <https://doi.org/10.1021/jasms.0c00386>, 2021.
- 483 Shen, J., Elm, J., Xie, H.-B., Chen, J., Niu, J., and Vehkamäki, H.: Structural Effects of Amines in Enhancing Methanesulfonic
484 Acid-Driven New Particle Formation, *Environ. Sci. Technol.*, 54, 13498-13508, <https://doi.org/10.1021/acs.est.0c05358>, 2020.
- 485 Shen, J., Xie, H.-B., Elm, J., Ma, F., Chen, J., and Vehkamäki, H.: Methanesulfonic Acid-driven New Particle Formation
486 Enhanced by Monoethanolamine: A Computational Study, *Environ. Sci. Technol.*, 53, 14387-14397,
487 <https://doi.org/10.1021/acs.est.9b05306>, 2019.



- 488 Silva, P. J., Erupe, M. E., Price, D., Elias, J., G. J. Malloy, Q., Li, Q., Warren, B., and Cocker, D. R.: Trimethylamine as
489 Precursor to Secondary Organic Aerosol Formation via Nitrate Radical Reaction in the Atmosphere, *Environ. Sci. Technol.*,
490 42, 4689-4696, <https://doi.org/10.1021/es703016v>, 2008.
- 491 Tan, W., Zhu, L., Mikoviny, T., Nielsen, C. J., Wisthaler, A., D'Anna, B., Antonsen, S., Stenström, Y., Farren, N. J., Hamilton,
492 J. F., Boustead, G. A., Brennan, A. D., Ingham, T., and Heard, D. E.: Experimental and Theoretical Study of the OH-Initiated
493 Degradation of Piperazine under Simulated Atmospheric Conditions, *J. Phys. Chem. A*, 125, 411-422,
494 <https://doi.org/10.1021/acs.jpca.0c10223>, 2021.
- 495 Thornton, J. A., Kercher, J. P., Riedel, T. P., Wagner, N. L., Cozic, J., Holloway, J. S., Dubé, W. P., Wolfe, G. M., Quinn, P.
496 K., Middlebrook, A. M., Alexander, B., and Brown, S. S.: A large atomic chlorine source inferred from mid-continental
497 reactive nitrogen chemistry, *Nature*, 464, 271-274, <https://doi.org/10.1038/nature08905>, 2010.
- 498 Veres, P. R., Neuman, J. A., Bertram, T. H., Assaf, E., Wolfe, G. M., Williamson, C. J., Weinzierl, B., Tilmes, S., Thompson,
499 C. R., Thames, A. B., Schroder, J. C., Saiz-Lopez, A., Rollins, A. W., Roberts, J. M., Price, D., Peischl, J., Nault, B. A., Møller,
500 K. H., Miller, D. O., Meinardi, S., Li, Q., Lamarque, J.-F., Kupc, A., Kjaergaard, H. G., Kinnison, D., Jimenez, J. L., Jernigan,
501 C. M., Hornbrook, R. S., Hills, A., Dollner, M., Day, D. A., Cuevas, C. A., Campuzano-Jost, P., Burkholder, J., Bui, T. P.,
502 Brune, W. H., Brown, S. S., Brock, C. A., Bourgeois, I., Blake, D. R., Apel, E. C., and Ryerson, T. B.: Global airborne sampling
503 reveals a previously unobserved dimethyl sulfide oxidation mechanism in the marine atmosphere, *Proc. Natl. Acad. Sci. U.S.A.*,
504 117, 4505, <https://doi.org/10.1073/pnas.1919344117>, 2020.
- 505 Wang, S. and Wang, L.: The atmospheric oxidation of dimethyl, diethyl, and diisopropyl ethers. The role of the intramolecular
506 hydrogen shift in peroxy radicals, *Phys. Chem. Chem. Phys.*, 18, 7707-7714, <https://doi.org/10.1039/C5CP07199B>, 2016.
- 507 Wang, S., Riva, M., Yan, C., Ehn, M., and Wang, L.: Primary Formation of Highly Oxidized Multifunctional Products in the
508 OH-Initiated Oxidation of Isoprene: A Combined Theoretical and Experimental Study, *Environ. Sci. Technol.*, 52, 12255-
509 12264, <https://doi.org/10.1021/acs.est.8b02783>, 2018.
- 510 Wang, S., Wu, R., Berndt, T., Ehn, M., and Wang, L.: Formation of Highly Oxidized Radicals and Multifunctional Products
511 from the Atmospheric Oxidation of Alkylbenzenes, *Environ. Sci. Technol.*, 51, 8442-8449,
512 <https://doi.org/10.1021/acs.est.7b02374>, 2017.
- 513 Wang, K., Wang, W. G., Fan, C. C.: Reactions of C₁₂-C₁₄ N-Alkylcyclohexanes with Cl Atoms: Kinetics and Secondary
514 Organic Aerosol Formation, *Environ. Sci. Technol.*, 56(8): 4859-4870, <https://doi.org/10.1021/acs.est.1c08958>, 2022.
- 515 Wu, R., Wang, S., and Wang, L.: New Mechanism for the Atmospheric Oxidation of Dimethyl Sulfide. The Importance of
516 Intramolecular Hydrogen Shift in a CH₃SCH₂OO Radical, *J. Phys. Chem. A*, 119, 112-117, <https://doi.org/10.1021/jp511616j>,
517 2015.
- 518 Xia, M., Peng, X., Wang, W.: Significant Production of ClNO₂ and Possible Source of Cl₂ from N₂O₅ Uptake at a Suburban
519 Site in Eastern China, *Atmos. Chem. Phys.*, 20(10): 6147-6158, <https://doi.org/10.1021/10.5194/acp-20-6147-2020>, 2020.



- 520 Xie, H. B., Ma, F.F., Yu, Q., He, N., and Chen, J. W.: Computational Study of the Reactions of Chlorine Radicals with
521 Atmospheric Organic Compounds Featuring NH_x - π -Bond ($x = 1, 2$) Structures, *J. Phys. Chem. A*, 121, 1657-1665,
522 <https://doi.org/10.1021/acs.jpca.6b11418>, 2017.
- 523 Xie, H. B., Li, C., He, N., Wang, C., Zhang, S., and Chen, J. W.: Atmospheric Chemical Reactions of Monoethanolamine
524 Initiated by OH Radical: Mechanistic and Kinetic Study, *Environ. Sci. Technol.*, 48, 1700-1706,
525 <https://doi.org/10.1021/es405110t>, 2014.
- 526 Xie, H. B., Ma, F.F., Wang, Y., He, N., Yu, Q., and Chen, J. W.: Quantum Chemical Study on $\cdot\text{Cl}$ -Initiated Atmospheric
527 Degradation of Monoethanolamine, *Environ. Sci. Technol.*, 49, 13246-13255, <https://doi.org/10.1021/acs.est.5b03324>, 2015.
- 528 Young, C. J., Washenfelder, R. A., Edwards, P. M., Parrish, D. D., Gilman, J. B., Kuster, W. C., Mielke, L. H., Osthoff, H. D.,
529 Tsai, C., Pikelnaya, O., Stutz, J., Veres, P. R., Roberts, J. M., Griffith, S., Dusanter, S., Stevens, P. S., Flynn, J., Grossberg,
530 N., Lefer, B., Holloway, J. S., Peischl, J., Ryerson, T. B., Atlas, E. L., Blake, D. R., and Brown, S. S.: Chlorine as a primary
531 radical: evaluation of methods to understand its role in initiation of oxidative cycles, *Atmos. Chem. Phys.*, 14, 3427-3440,
532 <https://doi.org/10.5194/acp-14-3427-2014>, 2014.
- 533 Yu, D., Tan, Z., Lu, K., Ma, X., Li, X., Chen, S., Zhu, B., Lin, L., Li, Y., Qiu, P., Yang, X., Liu, Y., Wang, H., He, L., Huang,
534 X., and Zhang, Y.: An explicit study of local ozone budget and NO_x -VOCs sensitivity in Shenzhen China, *Atmos. Environ.*,
535 224, 117304, <https://doi.org/10.1016/j.atmosenv.2020.117304>, 2020.
- 536 Yu, F. and Luo, G.: Modeling of gaseous methylamines in the global atmosphere: impacts of oxidation and aerosol uptake,
537 *Atmos. Chem. Phys.*, 14, 12455-12464, <https://doi.org/10.5194/acp-14-12455-2014>, 2014.
- 538 Yu, Q., Xie, H. B., and Chen, J. W.: Atmospheric chemical reactions of alternatives of polybrominated diphenyl ethers initiated
539 by OH: A case study on triphenyl phosphate, *Sci. Total Environ.*, 571, 1105-1114,
540 <https://doi.org/10.1016/j.scitotenv.2016.07.105>, 2016.
- 541 Yu, Q., Xie, H. B., Li, T., Ma, F., Fu, Z., Wang, Z., Li, C., Fu, Z., Xia, D., and Chen, J. W.: Atmospheric chemical reaction
542 mechanism and kinetics of 1,2-bis(2,4,6-tribromophenoxy)ethane initiated by OH radical: a computational study, *RSC Adv.*,
543 7, 9484-9494, <https://doi.org/10.1039/C6RA26700A>, 2017.
- 544 Yuan, B., Coggon, M. M., Koss, A. R., Warneke, C., Eilerman, S., Peischl, J., Aikin, K. C., Ryerson, T. B., and de Gouw, J.
545 A.: Emissions of volatile organic compounds (VOCs) from concentrated animal feeding operations (CAFOs): chemical
546 compositions and separation of sources, *Atmos. Chem. Phys.*, 17, 4945-4956, <https://doi.org/10.5194/acp-17-4945-2017>, 2017.
- 547 Zhang, R., Wang, G., Guo, S., Zamora, M. L., Ying, Q., Lin, Y., Wang, W., Hu, M., and Wang, Y.: Formation of Urban Fine
548 Particulate Matter, *Chem. Rev.*, 115, 3803-3855, <https://doi.org/10.1021/acs.chemrev.5b00067>, 2015.
- 549 Zhang, Z., Lin, L., and Wang, L.: Atmospheric oxidation mechanism of naphthalene initiated by OH radical. A theoretical
550 study, *Phys. Chem. Chem. Phys.*, 14, 2645-2650, <https://doi.org/10.1039/C2CP23271E>, 2012.
- 551 Zhao, Y. and Truhlar, D. G.: The M06 suite of density functionals for main group thermochemistry, thermochemical kinetics,
552 noncovalent interactions, excited states, and transition elements: two new functionals and systematic testing of four M06-class
553 functionals and 12 other functionals, *Theor. Chem. Acc.*, 120, 215-241, <https://doi.org/10.1007/s00214-007-0310-x>, 2008.



- 554 Zito, P., Dötterl, S., and Sajeва, M.: Floral Volatiles in a Sapromyiophilous Plant and Their Importance in Attracting House
555 Fly Pollinators, *J. Chem. Ecol.*, 41, 340-349, <https://doi.org/10.1007/s10886-015-0568-8>, 2015.